

AN ON-LINE ELECTRICAL RESISTANCE CORROSION MONITOR FOR STUDYING
CARBON STEEL CORROSION UNDER FEEDER PIPE CONDITIONS

Jointly Funded by

CNER and COG Working Party 15

By

D. Sun, L. Yang and F. Steward

Centre for Nuclear Energy Research
Fredericton, N.B.
E3B 6C2

ABSTRACT

An in-situ corrosion rate monitor using a carbon steel tube, a carbon steel rod or a carbon steel wire as the sensing element has been developed. The monitor was tested both in an inert system at room temperature and in a high-temperature and high-pressure loop with LiOH solution. Experimental results from the room temperature tests show that the amount of weight loss of the carbon steel sensing element calculated from the electrical resistance signal agrees well with the increase in the amount of iron dissolved into the solution. Experimental results from the high-temperature tests show that the corrosion monitor responded to the corrosion rate changes when air or sulfuric acid was added. The precision of the monitor under the simulated feeder pipe conditions was found to be $\pm 0.04 \mu\text{m}$ to $\pm 1 \mu\text{m}$ in terms of thickness change. The variation in precision is dependent upon the dimension of the sensing element.

Presented at
the 19th Annual Conference of the Canadian Nuclear Society
Toronto

1998 October

1.0 INTRODUCTION

Introduction

The flow accelerated feeder pipe wall thinning (corrosion) of the CANDU-6 reactors is a serious problem.^{1,2} Many efforts have been made to study the mechanisms involved in feeder pipe corrosion since the accelerated thinning was discovered. An on-line monitor to determine wall thinning with a precision in the order of 0.1 μm under feeder pipe conditions would be an ideal tool since this device could reduce the time required for the laboratory tests from months to weeks. This paper describes the development of a high precision on-line electrical resistance monitor for corrosion rate measurements under simulated feeder pipe conditions (LiOH solution, 5 to 20 m/s velocity, 310 °C temperature and 10.3 mPa pressure)³.

2.0 EXPERIMENTAL

2.1 The high-temperature recirculating loop

The high-temperature recirculating loop was described in references^{4,5}. The maximum flow in this loop was 0.6 L/min. Grab samples were taken periodically from the feed tank to determine the concentration of iron, chromium and other impurities. The concentrations of dissolved oxygen and hydrogen, conductivity, and pH of the solution were monitored continuously with on-line sensors.

2.2 The sensing elements

The monitoring device functions on the principle that the resistance of a carbon steel sensing element increases as the cross-sectional area of the sensing element decreases, due to corrosion. The sensing element is either a carbon steel wire, ~150 mm length x 0.75 mm diameter, a carbon steel rod, ~130 mm length x 2.0 mm diameter, or a carbon steel tube, ~50 mm length, 1 mm i.d. and 3.17 mm o.d. Figure 9 shows the schematic diagram for the wire and rod version monitors and Figure 2 shows the schematic diagram for the tube version monitor. Both the rod and the tube were machined from the wall of carbon steel grade A106B pipe, 2.5" (6.35 cm) o.d. The chemical composition of the carbon steel wire and the A106B pipe is given in Table 1.

Table 1 Chemical compositions of the carbon steel materials (wt%) analysed with Wavelength Dispersive Spectroscopy

	Cr	Ni	Mg	Mn	Zn	Co	Si	P	S
Wire	0.1	0.1	n.d.	0.65	1.74	0.1	0.22	0.61	0.1
A106B Pipe	0	n.d.	n.d.	0.83	n.d.	0.12	0.22	n.d.	n.d.

n.d.--not detectable(<0.02wt%)

For the rod and wire version, the rod or wire is inside a ceramic tube through which the liquid is forced to flow. In this way, the velocity of the fluid flowing around the sensing element could be varied between 5 and 20 m/s. Typical resistance values of the sensing elements at room temperature are 75 m Ω , 8.5 m Ω and 1.5 m Ω for the wire, rod and tube monitors, respectively.

Temperature compensation was achieved by using two Resistance Temperature Detectors (RTD), one placed up-stream and the other down-stream of the monitor. Both monitors and the RTDs were placed inside an oven.

The temperature dependence of the carbon steel sensing elements was determined experimentally in argon gas.

2.3 Instruments and data acquisition

A computer interfaced system for the resistance measurements and data acquisition was modified on the basis of the system used in the previous work⁵. The modified measuring system allows the measurements of the resistance in the range 0.5 to 1.5 m Ω to a precision of better than ± 0.5 $\mu\Omega$.

2.4 Experimental set-up for the calibration of the corrosion monitor at room temperature

To verify the response of the monitor to corrosion and to calibrate the signal of the corrosion monitor as a function of the weight loss of iron, a monitoring device with the stainless steel shell replaced by a plastic tube was tested in an iron-free recirculating system at room temperature. In this system, a glass beaker (1000 cc) was used as a reservoir for the solution where the pH was adjusted by adding 1 M H₂SO₄ or purging with fresh water. A peristaltic metering pump was used to circulate the solution through the carbon steel sensor. All tubing materials were made of Tygon. Samples were taken from the reservoir during the experiments and analysed for iron concentration by the atomic absorption spectroscopic method. The weight loss of the sensing element (iron) was calculated from the iron concentration data and compared with the weight loss calculated from the increase in the electrical resistance signal.

2.5 Experiments to test the conductivity effect on the measurements

To demonstrate that the current flowing through the solution between the two ends of a sensing element (carbon steel rod, tube or wire) during the resistance measurement was small, electrodes prepared from the carbon steel wire that was used as the sensing element in the corrosion monitor were dipped into 1 M sulfuric acid solution and a DC current was allowed to flow through the two electrodes. The voltage between the two electrodes was measured and the resistance was calculated using Ohm's law. This resistance should indicate approximately the resistance for the current to flow through the solution. Such a resistance is comprised of the ionic resistance of the solution and the electrochemical impedance at the interfaces between the electrodes and the solution.

3.0 RESULTS AND DISCUSSIONS

3.1 Temperature dependence of the resistivity of carbon steel sensing elements in an inert gas.

Figure 3 shows the measured resistivities for the carbon steel rod (A106B) and the carbon steel wire at different temperatures. The resistivities can be represented by second order polynomials:

$$\rho = 18.2515 + 0.05299t + 6.343 \times 10^{-5}t^2 \quad (1)$$

for the carbon steel rod (A106B), and

$$\rho = 19.9425 + 0.06049t + 6.7246 \times 10^{-5}t^2 \quad (2)$$

for the carbon steel wire. In Eqs. 1 and 2, ρ is in $\mu\Omega\text{-cm}$ and t is in $^{\circ}\text{C}$.

The results shown in Figure 3 are close to the reported value of 12-19 $\mu\Omega\text{-cm}$ for the carbon steel₆ with 0.3% to 0.5% carbon at 20 $^{\circ}\text{C}$.

3.2 The solution conductivity effect on the measurements of the electrical resistance signal

The resistance for the current flowing through the solution when a voltage is applied across a pair of electrodes in a beaker is given in Table 2.

Table 2 Resistance for the current flowing through the sulfuric acid solution

	Test #1	Test #2	Test #3	Test #4
Voltage (mV)	2.4	1.9	1.7	2
Resistance (Ω)	24	19	17	20

Notes: Current: 0.1 mA; H₂SO₄ concentration: 1 M; Depth of electrodes in solution: 2 cm; Distance between the two electrodes: 4.1 cm.

Table 2 shows that the resistance (electrochemical impedance at the two electrodes plus the solution resistance) for the current to go through the 1 M H₂SO₄ solution is in the range of 17 to 24 ohm which is approximately 270 times higher than that of the sensing elements (0.075 Ω). Therefore, the solution conductivity effect on the measurement of the resistance of the sensing element is not significant in the 1 M sulfuric acid solution. The solution conductivity effect is even smaller in the simulated PHT coolant, because the conductivity is significantly lower than that of the 1 M sulfuric acid solution.

3.3 The response of the electrical resistance of the monitor to corrosion at low temperature

The results from the low-temperature calibration experiments are shown in Figure 4. Before the acid was added or after the acid was purged, the pH of the solution (pure water) was approximately 7.0. When acid was added, the concentration of H_2SO_4 was about 0.1 M. Figure 4 shows that when the acid was added, both the electrical resistance of the monitor and the amount of iron dissolved into the solution increased. Up to the second purge of acid, the resistance change calculated based on the amount of iron dissolved into the solution agreed well with the measured electrical resistance change. This means that the weight loss of the sensing element (Fe) calculated based on the electrical resistance change agreed with the increase of dissolved iron in the solution assuming the amount of oxide on the surface of the sensing element is not significant. After the second purge, there was a small discrepancy, the measured resistance continued to rise while the calculated resistance remains unchanged. The cause for this discrepancy is not known. Figure 4 also shows that when no acid was added, or after the acid was purged, the increase of iron in the solution and the electrical resistance of the monitor remained essentially unchanged. Therefore, the electrical resistance signal can be used to predict the thinning rate of the carbon steel sensing element.

It should be noted that the corrosion rate after the first addition of the sulfuric acid was lower than that after the second addition. It is not known what caused such a difference in the corrosion rates. It is possible that this difference was caused by either variation in the flow rate through the monitoring device or a difference in the amount of sulfuric acid added.

3.4 Response of the corrosion rate monitor to the addition of air and the change in pH

Figures 5 and 6 show the responses of the carbon steel wire and the carbon steel rod monitors respectively, to the addition of air (by bubbling compressed air into the feed tank). Data were collected for a week pair. During the one-week period, the dissolved oxygen concentration was in the range of 30 to 40 ppb, and there was essentially no change in the resistances of the sensing elements. The noise of the signal was within $\pm 30 \mu\Omega$ for the wire monitor and $\pm 5 \mu\Omega$ for the carbon steel rod monitor. The corresponding precision in measuring the thickness change is $\pm 0.04 \mu\text{m}$ and $\pm 0.5 \mu\text{m}$ for the wire and rod monitors, respectively, in pH 9.5 LiOH solution at 310°C and 10.3 mPa.

Approximately 2 hours after the introduction of air, the pH changed from 9.5 to ~ 8 and the resistance of both the wire and the rod monitors started to increase rapidly. In 2.5 days, the calculated thickness change reached $0.8 \mu\text{m}$ for the wire monitor and $1.1 \mu\text{m}$ for the rod monitor.

The dissolved oxygen concentration measured by the Orbisphere at the down stream location (after cooling and depressurisation) was 350 ppb to 400 ppb after the addition of air. The difference between the oxygen concentration in the feed tank, ~ 8 ppm, and the oxygen concentration determined by the Orbisphere sensor was probably caused by the reaction of oxygen with the reducing species in the high temperature loop because the loop had previously been used with hydrogenated water. Thus the dissolved oxygen concentration in the loop where the corrosion monitoring device was mounted should be between 350 ppb and 8 ppm.

The pH change was probably caused by the CO_2 impurity (about 330 ppm according to the

manufacturer) in the compressed air. Prior to the addition of air, the dissolved iron concentration was between 2 and 7 ppb, which is approximately the same as the solubility⁷ of magnetite at 310°C. The dissolved iron concentration data was not available after the addition of air. However, the solubility of magnetite in the solution should have increased⁸ slightly when the pH changed from 9.5 to 8. Hence, the changes in both the pH and the electrochemical potential would cause an increase the corrosion rate of carbon steel materials.

Although the velocity of the fluid was higher around the wire sensing element (4.9 m/s) than the velocity around the rod sensing element (0.05 m/s), the thinning rate for the rod monitor was slightly higher than that of the wire monitor. This may be due to the differences in the chemical and metallurgical properties between the two carbon steel specimens or the difference in corrosion mechanism.

3.5 Response of the corrosion rate monitor to the addition of H₂SO₄

To accelerate corrosion and verify the response of the monitors, H₂SO₄ was added to the solution. Figures 7, 8 and 9 show the responses of the carbon steel rod monitor, the carbon steel tube monitor and the carbon steel wire monitor respectively, to the addition of H₂SO₄. The dissolved iron concentration and pH during the test period are shown in Figure 10. Figures 7 and 9 show that the electrical resistance signals of the two monitors increased immediately after the addition of H₂SO₄, and stopped about 10 hours later. It was observed that shortly after the addition of H₂SO₄, the dissolved iron concentration in the solution (Figure 10) increased to 12 to 15 ppm which is about the solubility⁷ of magnetite (15.5 ppm) in the solution at a pH of 3 and a temperature of 300°C. Hence corrosion was expected to slow down or stop because the solution became saturated with dissolved iron.

Figure 9 shows a response similar to those in Figures 7 and 8. However, the electrical resistance of the monitor did not stop increasing after the solution had been saturated with iron. It is not known if the difference in the behaviour of the wire monitor and the rod and tube monitors was caused by the difference in the chemical and metallurgical properties between the sensing elements.

The thickness change in response to the addition of H₂SO₄ was 7 µm for the rod monitor, 27 µm for the tube monitor and 2 µm for the wire monitor. Since the rod and the tube were machined from the same carbon steel pipe, the difference in the thickness change between the rod and the tube monitors was probably due to the difference in the flow velocities, 0.05 m/s for the rod and 2.1 m/s for the tube. However, the wire monitor, which was exposed to the highest flow, 4.9 m/s, showed the least thinning. Similar differences in thinning of the three monitors were observed during t carbon steel wire and the A106B pipe may have influenced the corrosion rates.

As mentioned in Section 3.4, the precision of the wire and the rod monitor were ±0.04 µm and ±0.5 µm respectively. The precision (or noise level) of the tube monitor was ±1 µm according to Figure 8. The reason for the higher precision with the wire monitor than with the tube monitor is that the electrical resistance was lower with the tube monitor (3 mΩ) than with the wire monitor (150 mΩ). In addition, the 3 mΩ resistance is at the low end of the 0 to 20 mΩ range of the

measuring system. A better precision could have been obtained if the tube signal was from 1 to 2 m Ω because, in this case, the next lower range, the 0 to 2 m Ω range, of the measuring system could be used.

3.6 Post test examination of the sensing elements.

The carbon steel rod and the carbon steel wire monitors were dismantled after the experiments. It was found that the sensing elements were uniformly corroded. No pitting was observed on the surface of the sensing elements after several months' operation in the high temperature loop. The connections between the silver leads and the extremities of the sensing elements were in good condition.

4.0 CONCLUSIONS

An in-situ corrosion rate monitor using a carbon steel tube, a carbon steel rod or a carbon steel wire as the sensing element has been developed. The monitor was tested both in an inert system at room temperature and in a high temperature and high-pressure loop with LiOH solution. Experimental results from the room temperature tests showed that the amount of weight loss of the carbon steel sensing element calculated from the electrical resistance signal agreed well with the increase in the amount of iron dissolved into the solution. Experimental results from the high-temperature tests showed that the corrosion rate monitor responded to the addition of air and sulfuric acid. The precision of the monitor under simulated feeder pipe conditions was found to be $\pm 0.04 \mu\text{m}$ to $\pm 1 \mu\text{m}$, depending upon the dimension of the sensing elements.

Acknowledgements

The Authors would like to express there thanks to:

Dr. R.A. Speranzini for the encouragement and support for this work, Drs. P.V. Balakrishnan, A.J. Elliot, L.W. Green and D.H. Lister for helpful technical discussions. T. Boutot and E. Macintosh for the assistances in the instrumentation. COG WP 15 for partial financial support for this work.

REFERENCES

1. K.A. Burrill and E.L. Cheluget, "The Connections Between Plant Data, Experimental Studies, and Mathematical Modelling of Flow Accelerated Corrosion (FAC) in The CANDU Primary Circuit", AECL draft report, August 1996.
2. D.H. Lister, J. Slade and N. Arbeau, "The Accelerated Corrosion of CANDU Outlet Feeders - Observations Possible Mechanisms and Potential Remedies", presented to the CNS Meeting, Toronto, June 1997.
3. D. Sun, L. Yang and F. R. Steward, "Development of an On Line Electrical Resistance Corrosion Monitor for Studying Carbon Steel Corrosion Under Feeder Pipe Conditions", COG Report, COG-97-451/RC-1947/CNER-97-02, August 1998.
4. L. Yang, J. Brake, D. Sun and F. Steward, "Development of a hydrogen Probe for CANDU Reactor Primary Heat Transport System", COG Report, COG-96-056, 1996.
5. L. Yang, X. Sun, F. Steward and D. Morris, "Measurements of Henry's Law Constant for Hydrogen in Water Utilizing a Palladium Differential Resistance Sensor", Ber. Bunsenges. Phys. Chem., 102, No.5, 1-6, 1998.
6. Electrical Engineer's Reference Book, 13th Edition, M.G. Say Edited, Butterworths, London, Page 2-12, 1977
7. F.H. Sweeton and C.F. Baes, Jr., "The Solubility of Magnetite and Hydrolysis of Ferrous Ion in Aqueous Solutions at Elevated Temperatures", J. Chem. Thermodynamics, 2, Page 479-500, 1970.
8. P.R. Tremaine and J.C. LeBlanc, "The Solubility of Magnetite and Hydrolysis and Oxidation of Fe^{2+} in Water to 300°C", J. Solution Chemistry, vol. 9, page 415-442, 1980.

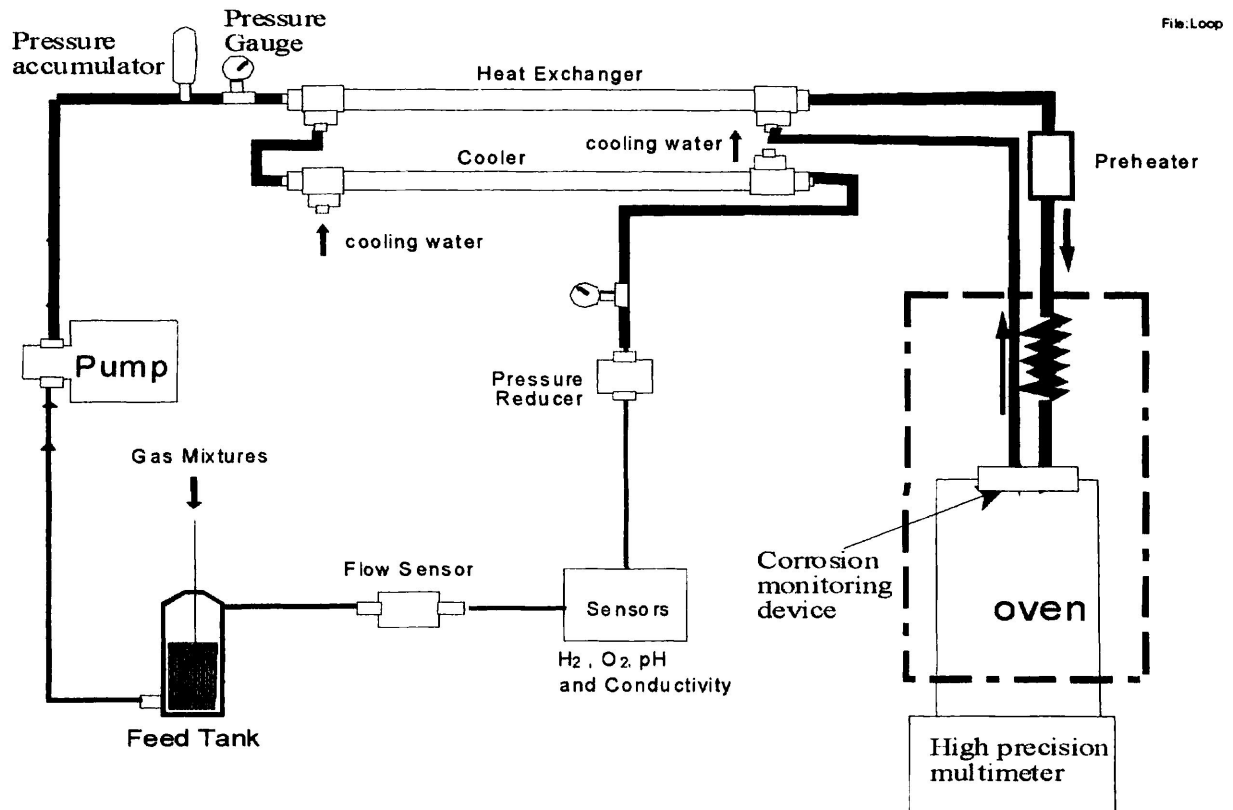


Figure 1 A schematic diagram of the high temperature loop

file: probe rod2

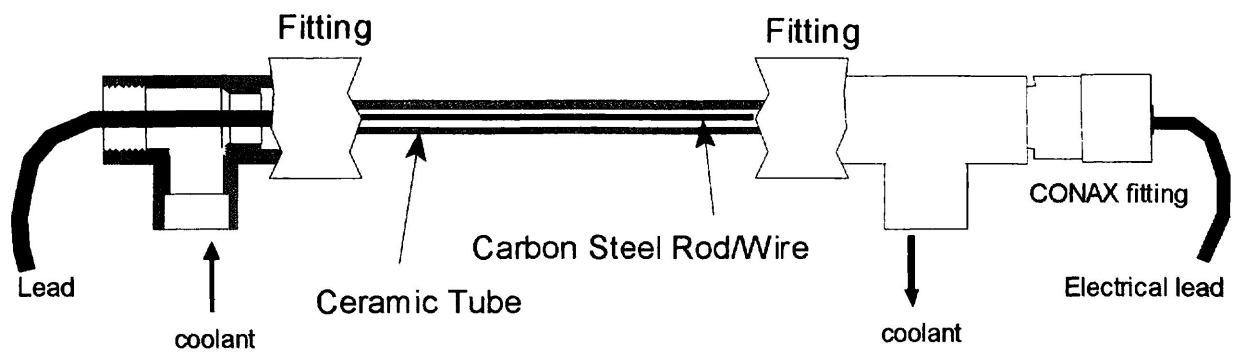


Figure 2 A schematic diagram of the rod and wire version carbon steel thinning rate monitor

file: probe-tub2

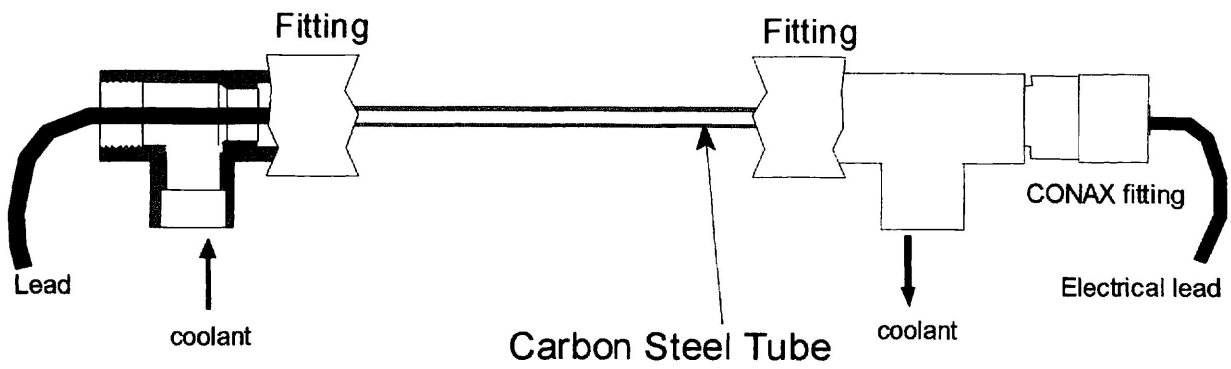
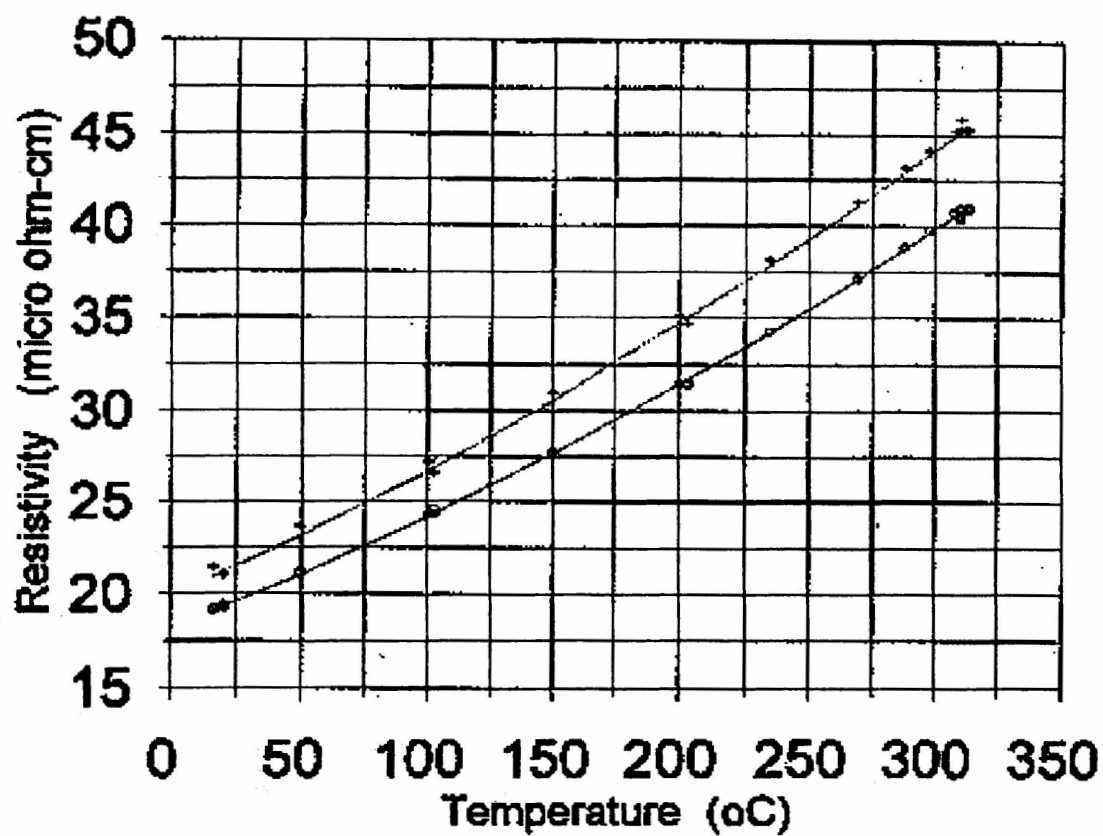


Figure 3 A schematic diagram of the tube version carbon steel thinning rate monitor



• rod monitor + wire monitor — curve fit, rod - - - - - curve fit, wire

Figure 4 The temperature dependence of the resistivity of the carbon steel sensing elements

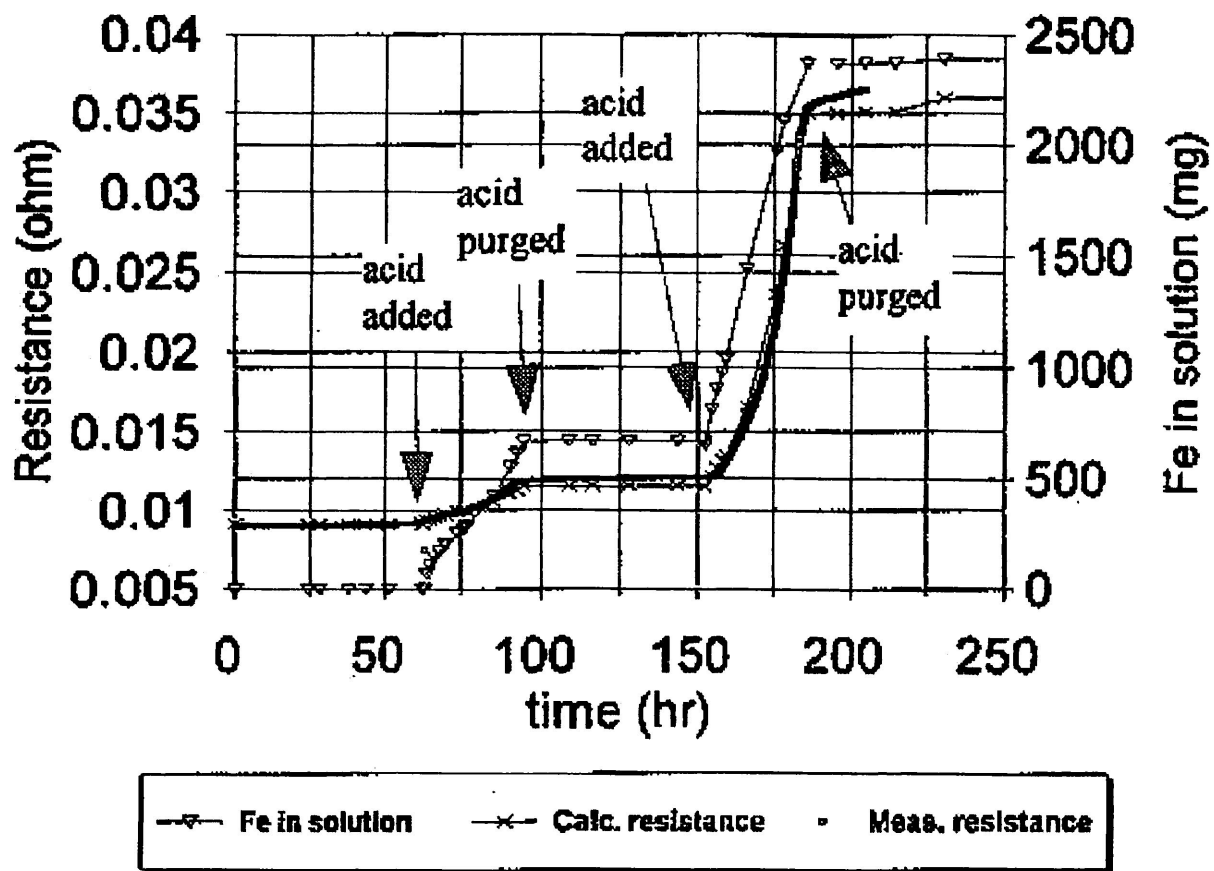


Figure 5 Comparisons between the electrical signal calculated based on the amount of iron lost into the solution and the measured electrical signal at 25 °C.
Sensing element: 2 mm diameter carbon steel (A106B) rod.

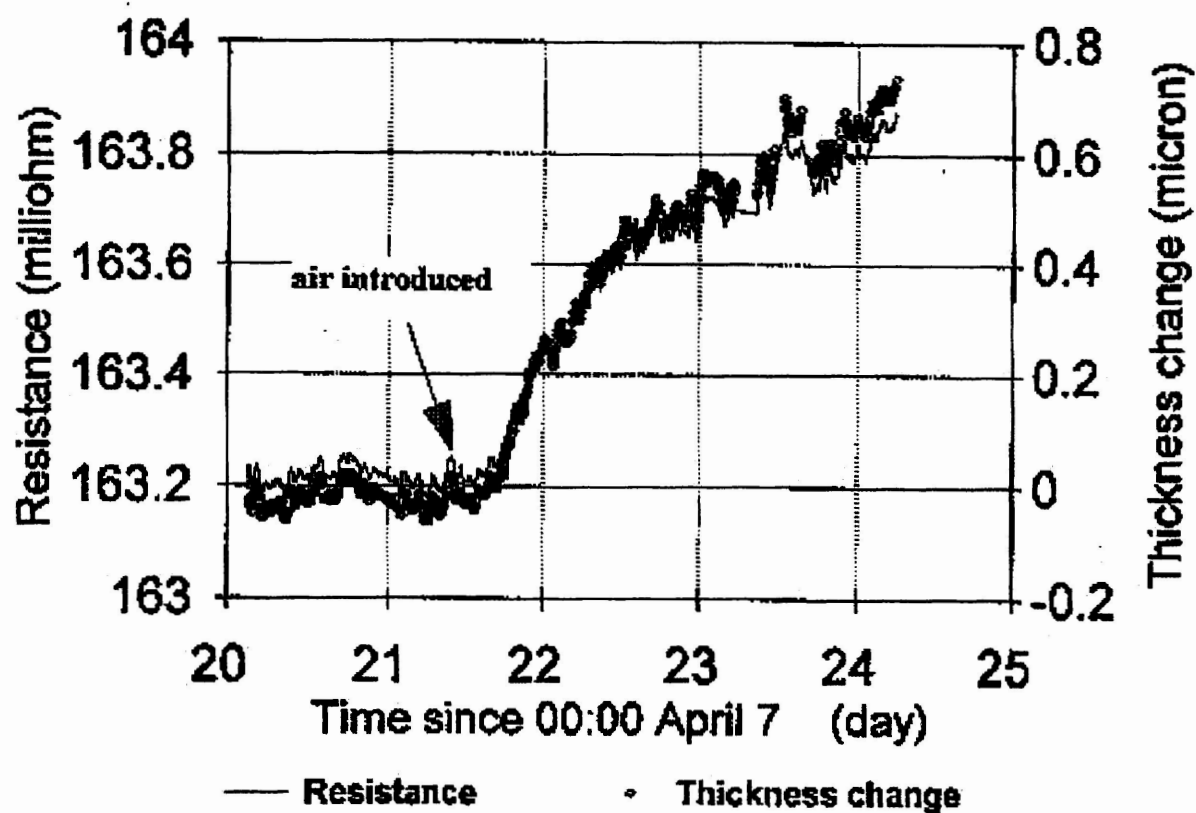


Figure 6 The response of the corrosion rate monitor to the addition of air into the LiOH solution at 310°C, using a carbon steel wire as the sensing element . After air addition, pH changed from 9.5 to 8 and dissolved O₂ changed from 35 ppb to >350 ppb; Fluid velocity: 4.9 m/s; Diameter of the wire: 0.75 mm.

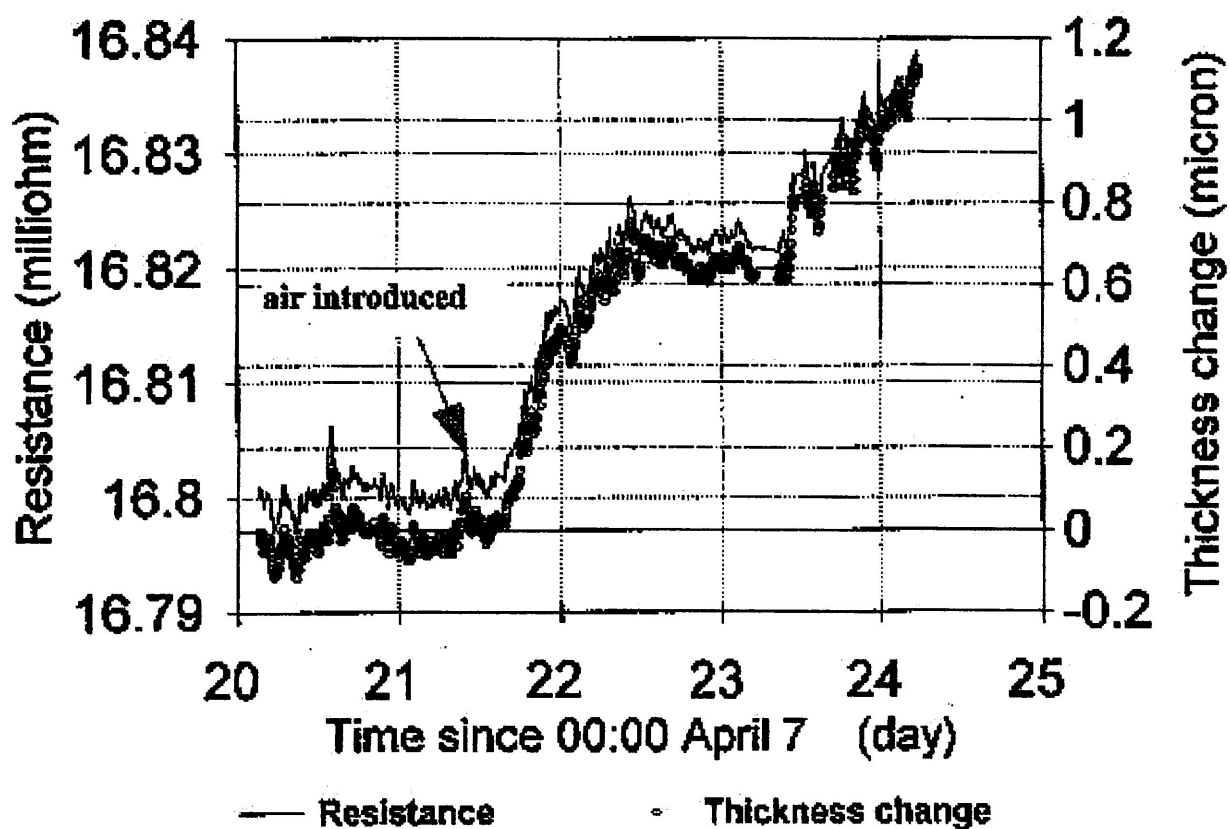


Figure 7 The response of the corrosion rate monitor using a carbon steel rod (A106B) as the sensing element to the addition of oxygen into the LiOH solution at 310°C. After air addition, pH changed from 9.5 to 8 and dissolved O₂ changed from 35 ppb to >350 ppb; Fluid velocity: 4.9 m/s; Diameter of the wire: 0.75 mm.

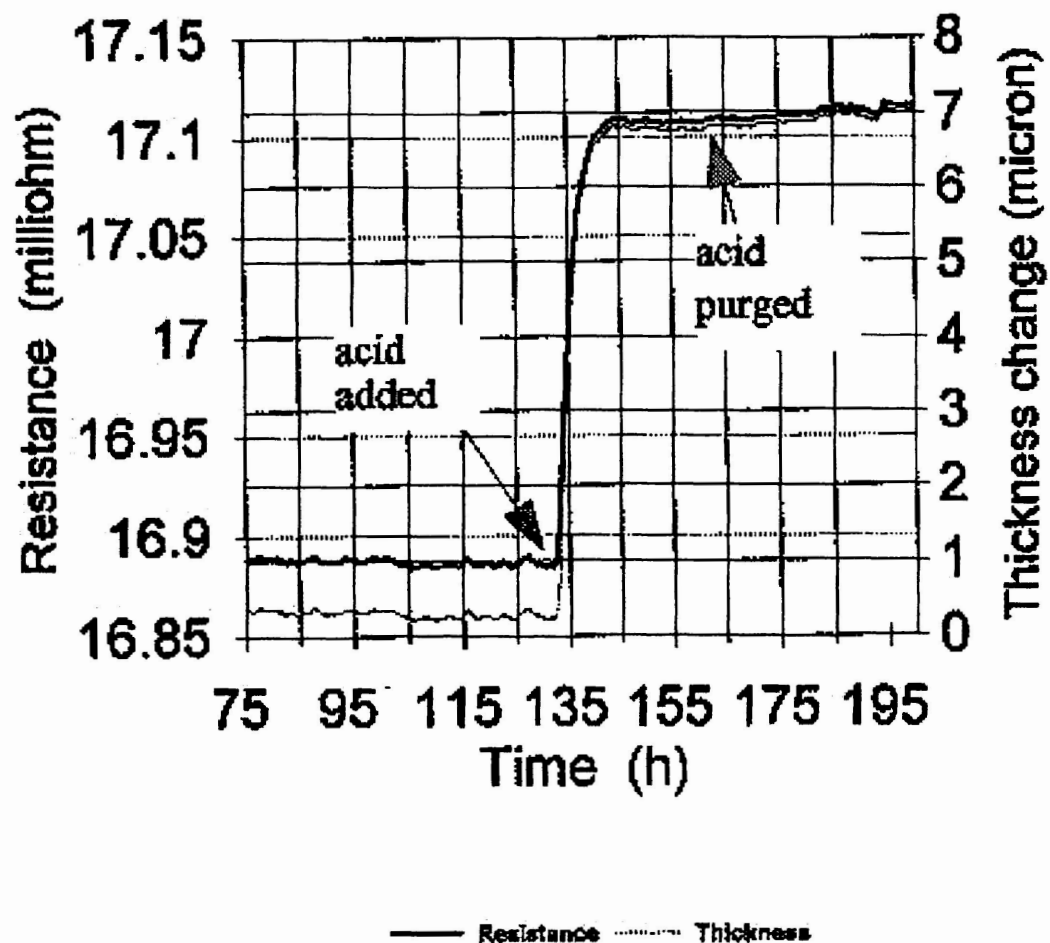


Figure 8

The response of the corrosion rate monitor to the addition of H_2SO_4 into the LiOH solution, using a carbon steel rod (A106B) as the sensing element
 Temperature: 311 °C; Dissolved O_2 : 30 to 40 ppb; Fluid velocity: 0.05 m/s;
 Diameter of the rod: 2 mm; pH and dissolved iron concentration see Figure 10.

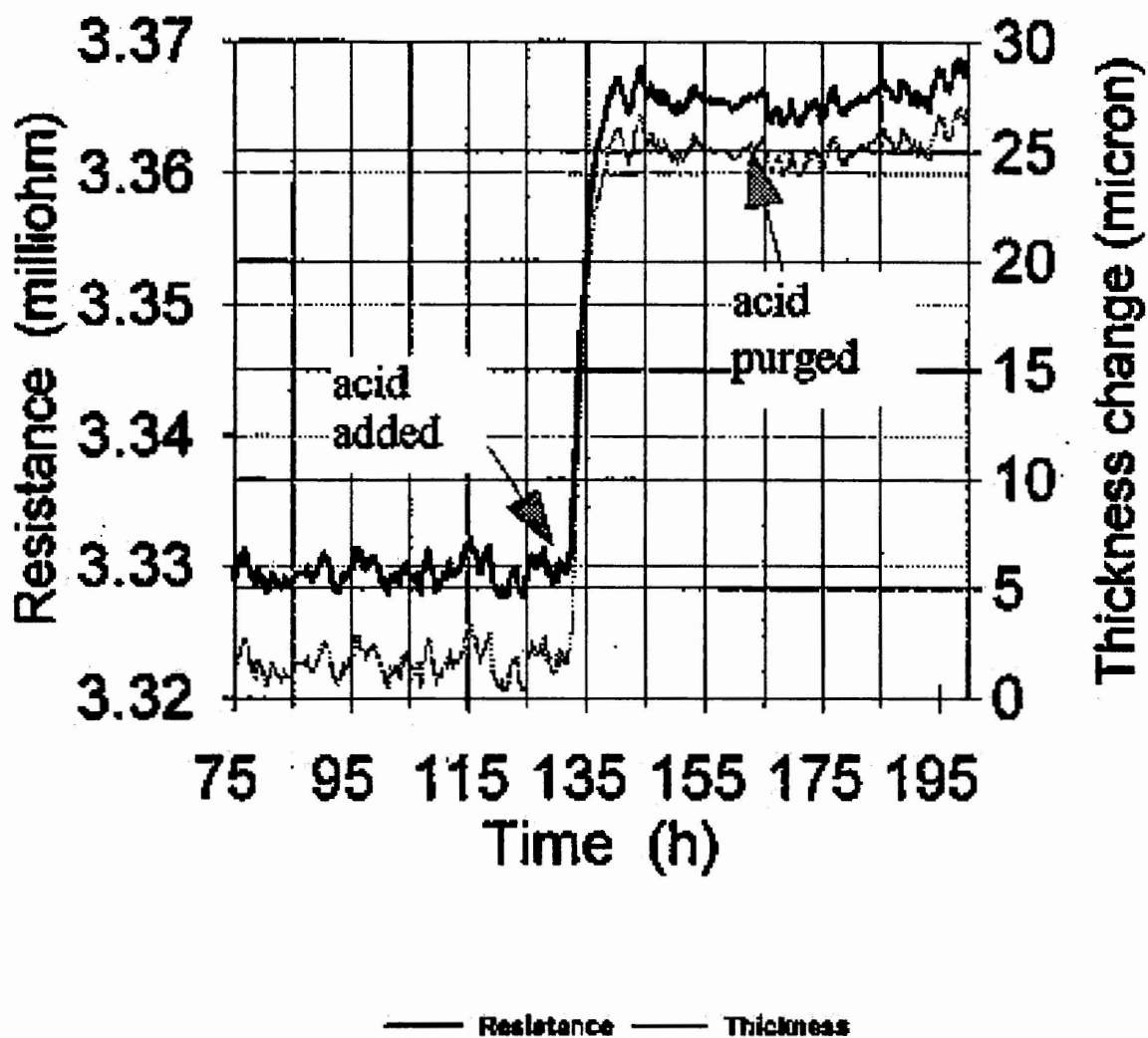


Figure 9

The response of the corrosion rate monitor to the addition of H_2SO_4 into the $LiOH$ solution, using a carbon steel tube (A106B) as the sensing element.
 Temperature: $311\text{ }^{\circ}C$; Dissolved O_2 : 30 to 40 ppb; Fluid velocity: 2.1 m/s; Inside diameter of the tube: 1 mm; pH and dissolved iron concentration see Figure 10.

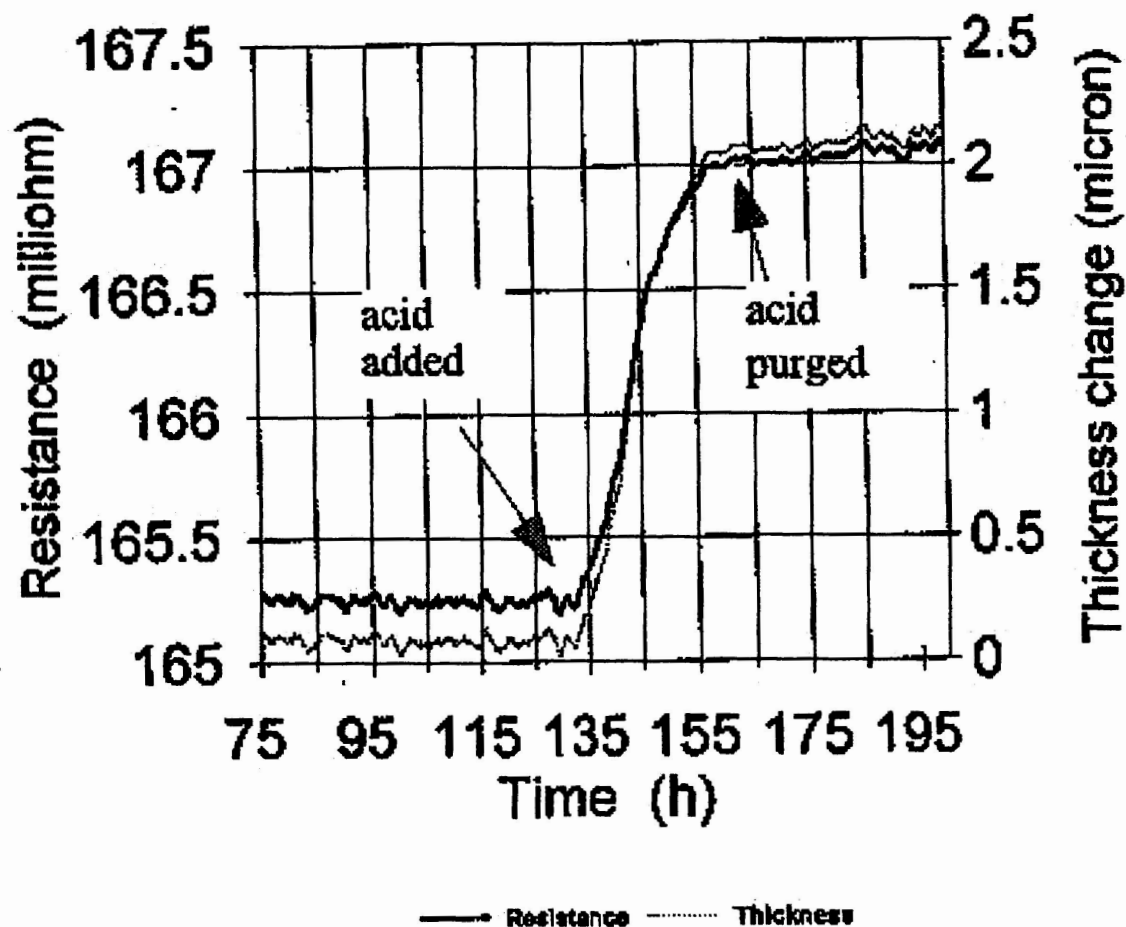


Figure 10 The response of the corrosion rate monitor to the addition of H_2SO_4 into the LiOH solution, using a carbon steel wire as the sensing element.
 Temperature: 311°C ; Dissolved O_2 : 30 to 40 ppb; Fluid velocity: 4.9 m/s;
 Diameter of the wire: 0.75 mm; pH and dissolved iron concentration see Figure 9.

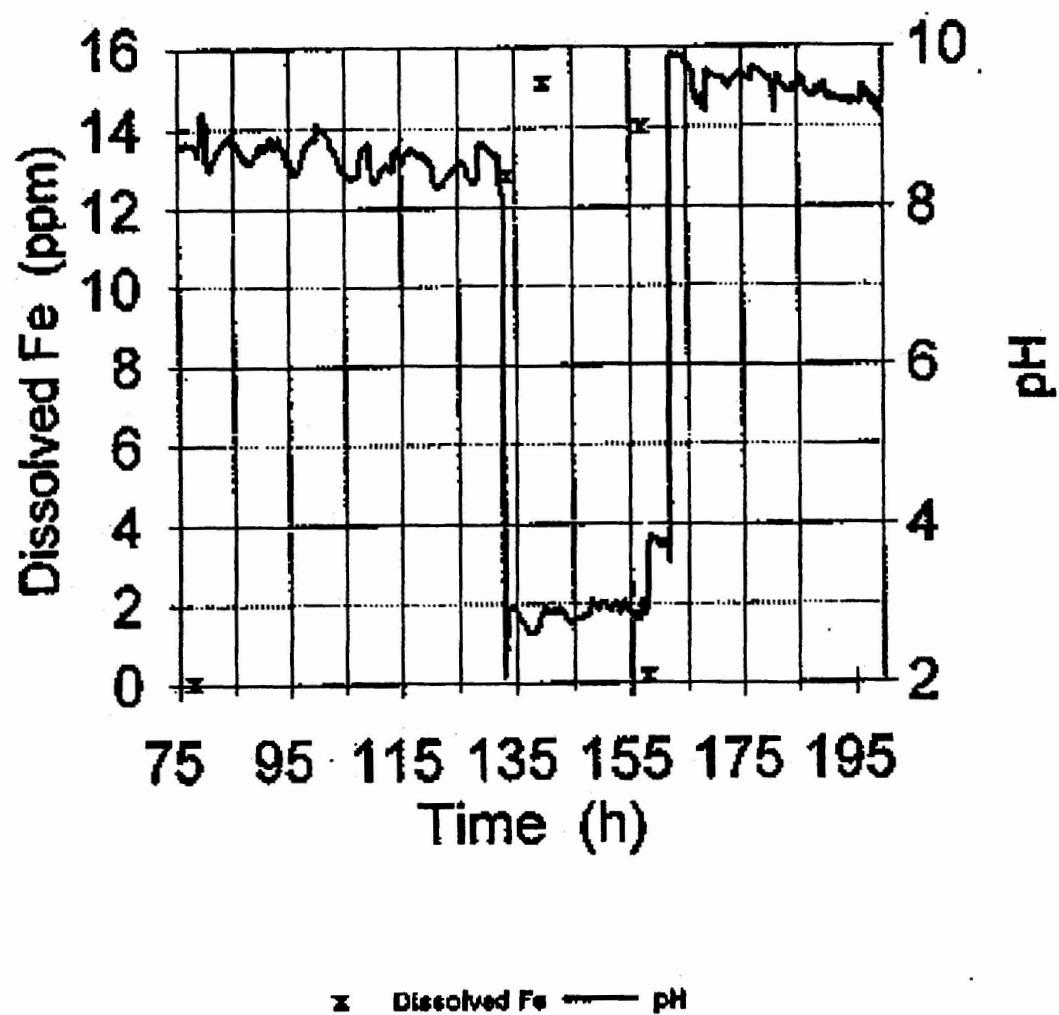


Figure 11 The dissolved iron concentration and pH in the solution during the experiments presented in Figures 7, 8 and 9.